Principal Investigator: Professor Janet Rankin
Institution: Brown University - Providence, RI 02912
Title: "In situ Transmission Electron Microscopy Heating Studies of Particle Coalescence and Microstructure Evolution in Nanosized Ceramics"
Grant No.: DE-FG02-95ER45542

Final Report

This report is divided into sections corresponding to the main areas of research for this grant: ***A. particle shape changes and stress effects,*** *and* ***B. novel infiltration techniques in the processing of alumina-based ceramics*** fabricated from nano- and sub-micron powders in order to minimize grain growth and maximize the final density in bulk samples.

A. Particle Shape Changes and Stress Effects

A.1. In situ TEM investigations

During the previous funding cycle, significant progress has been made towards an understanding of the relationships between initial particle shape and particle-particle contact geometry, and the ways in which individual particles and particle-pairs progress toward their lowest energy configurations. Specifically, previous work shows that individual particles behave quite differently than expected, and that their behavior is highly dependent on the existence (and presumably, precise nature) of internal and surface defects. Our work shows that isolated particles which are defect free, do not change shape in any appreciable way when subjected to *in situ* heating. An example is shown in Fig. 1. Here, an isolated particle of ZrO_2 is shown at room temperature and after heating at 850 °C for 2 hours. There is no observable difference between the two images. Significant effort has been made to understand the mechanisms responsible for these observations. Theoretical findings are discussed in section *A.1.a* Additional work on contacting oxide particles has also been published in several of our papers.[1, 2, 3]

DISCLAIMER

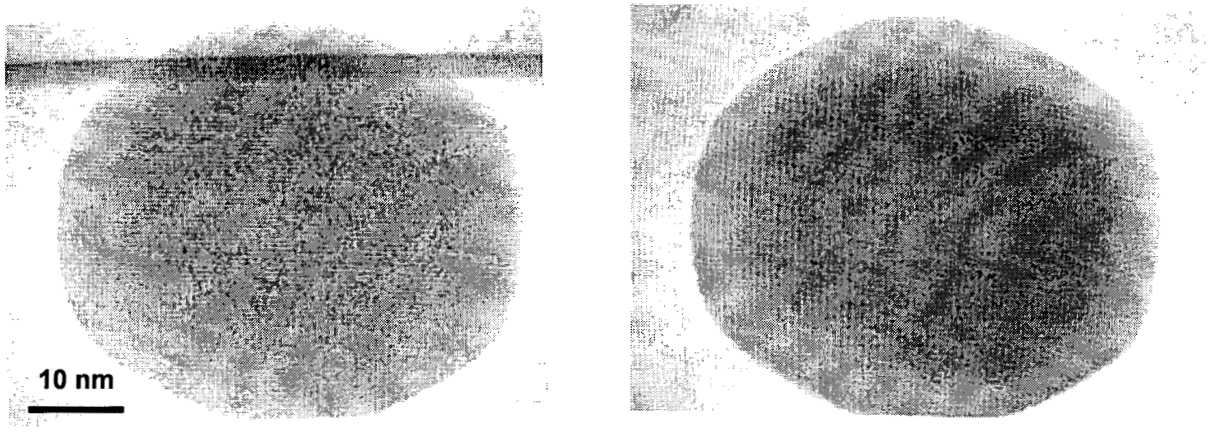

Figure 1. An isolated particle of ZrO_2 is shown at room temperature (left) and after heating at 850 °C for 1 hour (right). There is no observable difference between the two images.

In addition, recent findings suggest that the behavior of *particle pairs* is found to be linked to the presence of grain-boundaries, in particular, the orientation, and contact geometry of the coalescing particles. An example of this is shown in Fig. 2, which shows a series of images taken during the heating of a system of silicon particles with defects present. The images in Fig. 2 show highly irregular coalescence.

Systems of two distinct phases have also been investigated. This work has focused on the Al_2O_3/ZrO_2 system. Here, preliminary results show extremely interesting morphology evolution. Fig. 3 shows a high-resolution TEM image of a ZrO_2 particle on a larger Al_2O_3 particle. The system has been heated to 1600 °C for 4 hours (*ex situ*). Here, it can be seen that the zirconia particle is partially facetted, but the extent of faceting is much greater on vacuum/ZrO_2 surfaces than it is on zirconia surfaces in contact with the alumina. It is of interest to further examine this observation (typical of all Al_2O_3/ZrO_2 samples observed, regardless of extent or degree of heating). Preliminary calculations strongly suggest that the differences in grain-boundary morphology are not merely the result of kinetic limitations.

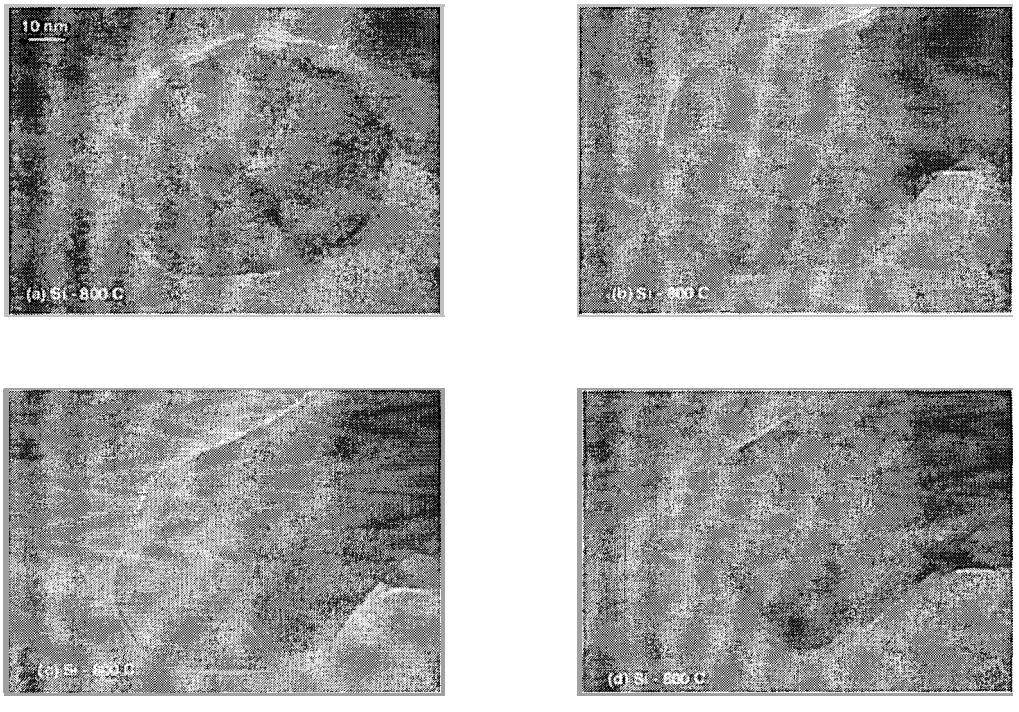

Figure 2 (a)-(d). A series of images taken during the heating of a system of silicon particles at 550 °C. The system contains at least one grain boundary.

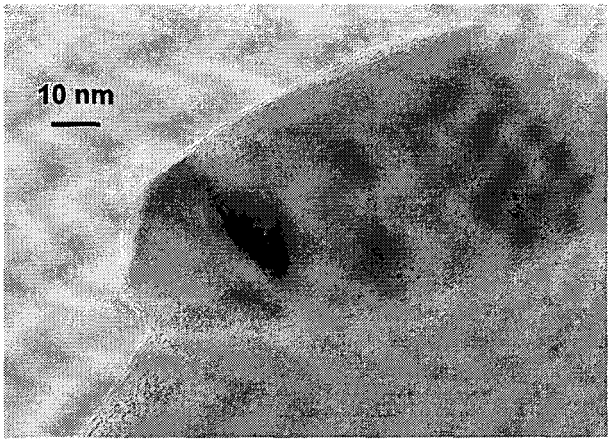

Figure 3. High-resolution TEM image of a ZrO_2 particle on a larger Al_2O_3 particle. The system has been heated to 1600 °C for 4 hours (*ex situ*). Note that the ZrO_2 particle is partially facetted, but the extent of faceting is much greater on vacuum/ZrO_2 surfaces than it is on ZrO_2 surfaces in contact with the alumina.

In prior TEM work, we have also shown that the energy barrier associated with forming new atomic steps can have a significant influence on particle morphology changes.[3] One example of this is that the step energy barrier will keep isolated particles from reaching their ECS. In contacting particles, this prior work also shows that step energy barriers can alter inter-particle neck formation and promote desintering. These effects are described in more detail in the next section.

A.2. The Influence of Atomic Steps on Particle Morphology Changes

The formation of a new monolayer on a faceted surface is depicted in Fig. 4. This process requires the formation of an atomic step. The excess energy associated with this step leads to the energy barrier cited in the previous paragraph. Note that the rounded corners and edges of crystalline particles are atomically rough, while faceted surfaces are atomically smooth. The rough, rounded surfaces are typically conceptualized as a collection of steps with heights on the order of an atomic spacing. These surfaces are more entropic, with atoms moving readily from one bonding position to another (e.g., from one atomic plane to another for atoms on a square lattice). Previous *in situ* TEM heating experiments provide direct evidence of this type of atomic scale motion in small particles[4,5] (similar observations on larger crystalline surfaces have also been made in more recent scanning tunneling microscopy studies). This type of atom "hopping" is usually much less prevalent on faceted surfaces where there is a nucleation energy barrier associated with the creation (or removal) of a stable atomic step. Following the original pioneering work of Burton, Cabrera, and Frank, the step energy barrier for forming a new monolayer island increases as the driving force decreases.[6] Thus, the step energy barrier is not that large

in a vapor deposition process with a high driving force (i.e., a high vapor phase supersaturation).

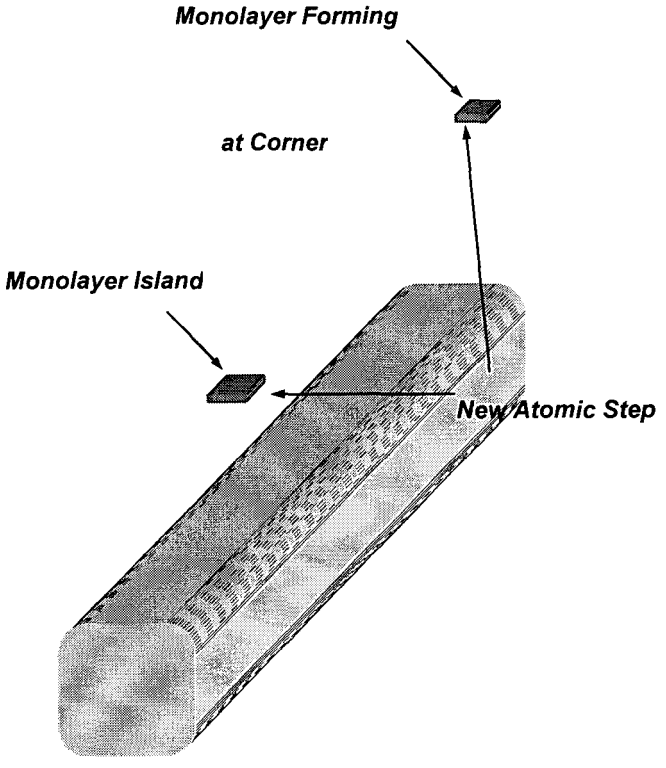

Figure 4. Schematic showing the formation of new atomic layers on a faceted surface. Compared with the island in the middle of the facet, the island in the corner has a lower nucleation energy barrier because it requires the formation of an atomic step with a shorter length.

However, shape changes in individual particles or during coarsening are driven only by curvature (or weighted mean curvature) effects. In all but the smallest particles, this means that the driving force is small and the step energy barrier is large (e.g., $> 40\ kT$, where k is Boltzmann's constant).[Error! Bookmark not defined., 7] Therefore, the step energy barrier should have a significant effect on morphology changes in particles that do not contain dislocations (i.e., because dislocations create steps when they intersect the particle surface). These large step energy barriers are consistent with our *in situ* TEM heating studies on isolated 100-200 nm MgO and ZrO_2 particles, where shape changes do not occur.[1, 2]

The nucleation barrier associated with removing an atomic layer is harder to visualize than the more traditional nucleation barrier for layer formation. Some analyses assume that this barrier is nonexistent.[8] Rohrer and Mullins note that the removal of a patch of material from the middle of a facet

is essentially equivalent to the formation an island, and thus has the same type of nucleation barrier.[7] Another perhaps more realistic model that we proposed is that a step originally located in the round corner region moves across the facet as material is removed.[Error! Bookmark not defined.] This behavior for a two-dimensional particle is shown in Fig. 5, where the corresponding step motion occurs in one dimension. Our previous analysis addresses this problem, and predicts that there is an energy barrier associated with removing the layer.[3] The cause of the energy barrier may not be immediately apparent, since a new step is not being created. However, moving a step from the rounded surface to the faceted surface will increase the energy of the system because of step-step interactions.[Error! Bookmark not defined.]

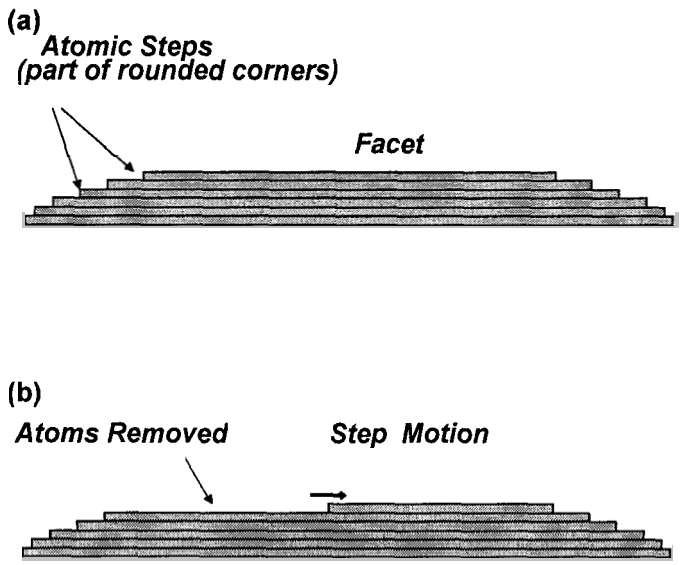

Figure 5. (a) Facet consists of a complete atomic layer, and rounded corners consist of atomic steps. (b) Removal of atoms causes the top step to move across the facet (to the right).

Traditional models of particle shape changes do not account for the step energy barrier associated with adding or removing additional atomic planes from a faceted surface. However, as noted above our experiments have demonstrated the importance of these effects, and we have analyzed several problems of this type in recent papers.[3, Error! Bookmark not defined.] Our results show that the formation and motion of atomic steps causes actual morphology changes to differ substantially from continuum models. This general conclusion applies to both "nanosized" particles, and to the somewhat larger particles that have been investigated in most of our experiments. Several other recent experimental studies which support our analysis of step-energy effects are also noted in a recent paper by Rohrer *et. al.*.[Error! Bookmark not defined.]

The analysis in one of our recent papers considers coarsening (or "Ostwald" ripening) processes

where the particle surfaces consist of both faceted and non-faceted regions.[Error! Bookmark not defined.] These problems have been studied theoretically for many years.[9,10,11,12] The majority of this previous work focuses on spherical particles with isotropic surface free energies. Another limitation of traditional coarsening models is that the descriptions of interface motion do not incorporate many of the kinetic effects that are associated with individual atomic steps. However, the free energy changes associated with coarsening appear to be too low to overcome this step energy barrier in dislocation-free particles (unless the particle size is very small). Our analysis demonstrates that the restrictions on step formation impose significant limitations on coarsening in faceted, dislocation-free particles. This can lead to behavior which differs significantly from traditional coarsening models. A paper has resulted from this work.[13]

A.3 Stress Effects and Computational Fourier Transform Moiré (CFTM) Techniques

Computational Fourier Transform Moiré (CFTM) techniques were used to detect and quantify strain contributions from edge and corner energies to the equilibrium shape of nano-sized particles of silicon and zirconia.

Computational Fourier Transform Moiré is a relatively novel approach for qualitatively studying crystalline defects and nanostructures. This method uses a HRTEM image, and produces the 2D displacement field defined over the whole image. The extraction of the displacement field requires 3 steps. The first is an image processing step in which a histogram equalization is applied to the original image in order to improve its contrast. Next, the image is analyzed through a digital Fourier-type technique to yield a continuous displacement field. Finally, the noise that affects this measured field is filtered out through a finite element-based smoothing algorithm. This last step insures that the resulting field is an elastic field which satisfies equilibrium and compatibility. The resulting displacement field is then used to compute strains, stresses and the stored elastic energy in the crystalline defects within the image. Thus, this technique is capable of supplying valuable information about the structure and energy of the lattice imperfection.

The CFTM procedure was originally proposed by Choi *et. al*,[14] where it was used to investigate the displacement field about a Frank partial in a ZnTe thin film. Later, Picu et al.[15] and Picu and Kim [16] applied the method to study the core structure and dilatation of a Lomer dislocation in Si-Ge. Previous work deals with highly non-homogeneous fields about crystalline defects, however, the method will work equally well in defect-free structures, and in structures where the defect is the surface.

Currently, the Wulff Construction accounts for only the surface energies as a function of

orientation. It is logical to expect that the region (a line where 2 facets meet, or a point where 3 facets meet) will have a different energy than that of the intersecting facets. It has been suggested that the edge energies may contribute significantly to the equilibrium shapes of small particles. This "extra" energy has been alluded to in previous studies,[17,18] however, we believe that Moiré Interferometry provides conclusive evidence of the existence, and extent of edge-energies.

Figure 6(a) shows an atomic resolution image of a zirconia nano-particle in a <101> projection. The particle, which was neither heat treated nor subjected to sintering, has developed well defined facets separated by curved surface regions. As discussed above, the surface energy associated with the non-flat zones is likely to induce strain energy in the particle and this should reflect in the ordering of the underlying lattice. To measure such an effect we used a 1D version of the CFTM method. In this we apply the same Fourier analysis as in the "standard" 2D CFTM, in one dimension, on data obtained from linear scans of the original image. To determine the effect of the corner/edge region 1 in Fig. 6(a), two linear paths were chosen for scanning. Figure 6(b) shows the relative displacements of the lattice when scanned along lines 1 and 2 in Fig. 6(a). It should be noted that these curves are relative displacements only, and that a constant rigid-body displacement was subtracted from each. In Fig. 6(a), the x-axis is normalized by the interplanar spacing along the [020] direction while the y-axis is arbitrary. The non-homogeneous deformation indicated by the curves in Fig. 6(b) is most likely due to the gradient of the surface energy in the respective regions. The exact relation between the measured strain and the surface chemical potential distribution will be investigated through a more involved 2D CFTM analysis.

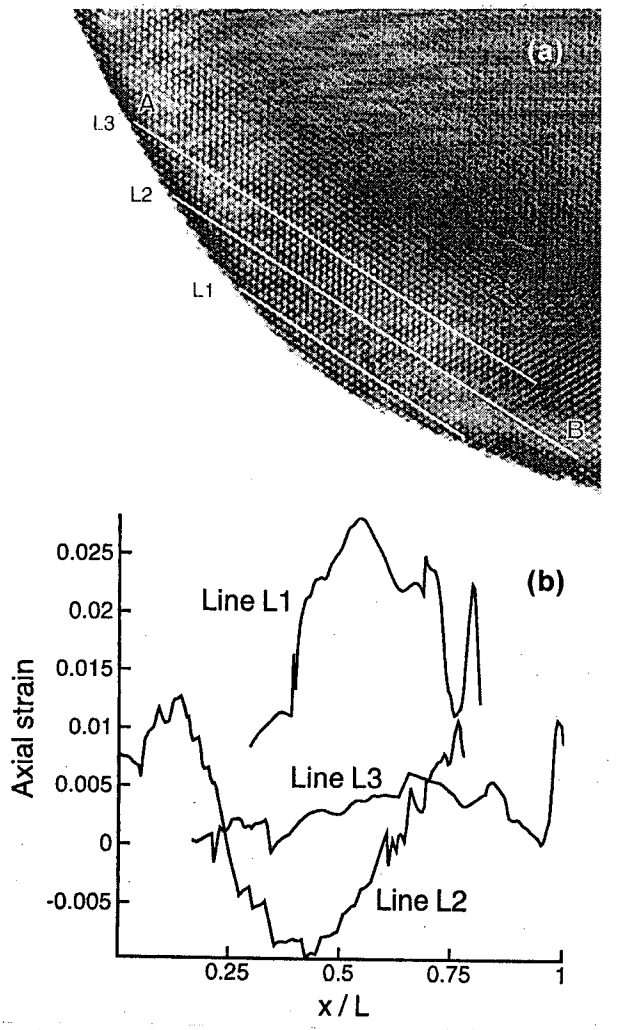

Figure 6. (a) HRTEM image of a ZrO_2 particle in a [101] projection. (b) Strains measured along lines L1, L2, and L3 in Fig. 6(a). The x-axis is normalized by the interplanar spacing along the [020] direction, while the y-axis is arbitrary.

As observed by a number of authors,[19,20] nano-particles smaller than a certain critical size undergo spontaneous solid state transformations (twinning) that distort the lattice. The phenomenon is assumed to be due to the non-uniform distribution of surface energy which, when the number of surface atoms represents a significant ratio of the total number of atoms in the particle, induces lattice reorganization for total energy minimization. An example of such highly deformed particle is shown in Fig. 7. This is a [110] projection of a Si particle that contains a number of twinned regions (one such region is marked

with the letter "A") as well as a regular lattice (marked by the letter "B") bounded by a single facet. The twinning transformation that occurred in Region "A" has induced an accommodation shear strain in the matrix (Region "B"). Apparently, the resulting shear stress overcame the Peierels stress and part of the strain energy was relaxed by the nucleation and propagation of a set of 60° dislocations These dislocations are dissociated into a 30° and a 90° partials of which the last one is trapped in the interface and has contributed to the shear strain accommodation. The mobile 30° partial advances in the matrix to a point at which the effect of the residual shear stress balances that of the stacking fault that separates the two partials associated with a given dislocation.

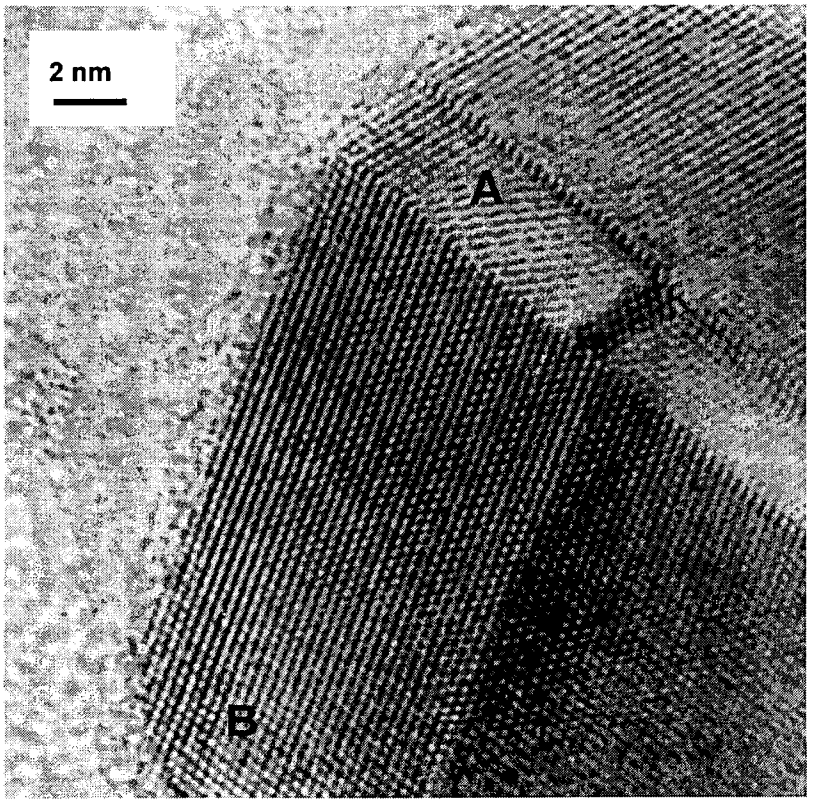

Figure 7. A [110] projection of a Si particle that contains a number of twinned regions (one such region is marked "A") as well as a regular lattice (marked "B") bounded by a single facet. The twinning transformation that occurred in Region "A" has induced an accommodation shear strain in the matrix.

It is interesting to note that the lattice close to the interface is rotated 6-7° with respect to the matrix far from the interface due to the proximity to the transformed region. This, corroborated with the known Burgers vector of the 30° partial and the measured spacing between the glide planes containing the dislocations (4-5 spacings in [112]), indicate the magnitude of the shear stress before the dislocations came in which gives an upper bound for the Peierels stress in Si. Further, the exact location of the 30° partials gives information about the interaction of these entities and about the departure of this interaction from that prescribed by elasticity theory. Such a departure would be due to the non-linearity and non-locality associated with the core, as shown by atomistic simulations performed in simpler bounded materials.[21]

B. Novel Infiltration Techniques to Suppress Grain Growth

B.1 Chemical Vapor Infiltration into the partially sintered pore structure of Al_2O_3 (Si_3N_4/Al_2O_3)

This work was an ongoing component of this grant. We have made significant strides in the understanding and control of gas-phase reactions to inhibit grain growth in sub-micron alumina, and have also extended this work to nanoscale alumina powders. The motivation and experimental details have been discussed in past continuation reports and published journal articles.[22,23] Samples infiltrated with SiH_4 and NH_3 often show inhibited grain growth in interior regions, with abnormal grain growth near the outer surface. A major obstacle to an improved understanding of the mechanisms involved in the observed grain growth suppression additions has been the inability to detect the existence and location of a Si_3N_{4y} -related phase or composition shift. At Brown, both EDS and EELS were previously used to investigate the chemical compositions of the grain-boundaries in the suppressed growth region of the Si_3N_{4y} infiltrated specimens, however, none of the spectra collected with these techniques showed any conclusive evidence of Si or N after sintering. To determine if Si and/or N was present in the infiltrated samples, samples were analyzed at Max Planck Institute, in a VG HB 501 STEM with a 0.26 nm probe size. Figure 8 shows EDS data collected in the suppressed grain growth region (approximately 450 nm from the edge of the pellet). There is no evidence of Si in the grain interiors, while an average Si concentration of 2 atomic percent was measured along the grain boundaries. The corresponding EELS spectra do not show any evidence of nitrogen at the grain boundaries or in the grain interiors.[23]

In the abnormal grain growth region, TEM images from Max Planck show the presence of a glassy phase at *some* of the grain boundary junctions (see Fig. 9). EDS scans of the amorphous glassy phase located at the grain boundaries and triple junctions confirm the presence of Al and Si. From the relative intensity values of these scans, the ratio of Si to Al in these pockets is ~2:1. The silicon content along grain boundaries in this region is approximately 10 atomic %.

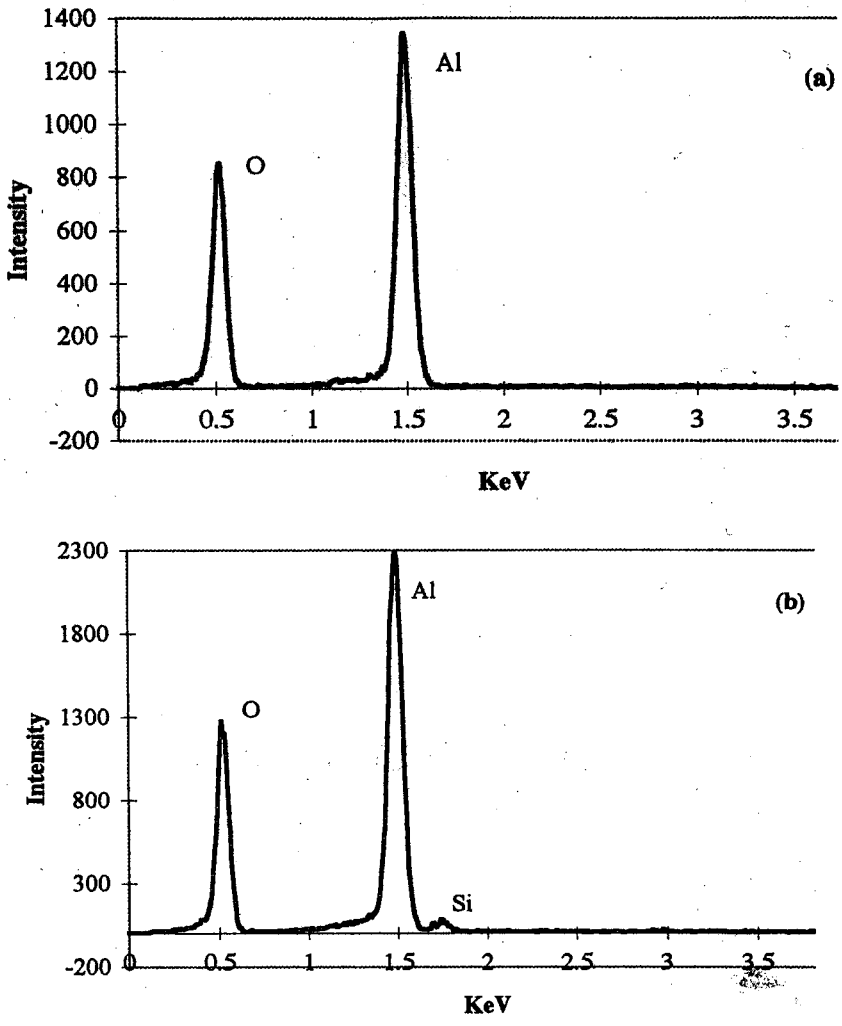

Figure 8. EDS scans in a region that exhibits suppressed grain growth (performed at Max Planck Institute). (a) grain interior, no Si detected. (b) grain boundary, Si detected (peak at 1.75 KeV).

SEM images of the infiltrated submicron alumina pellets suggest that the Si/N ratio must fall within an acceptable range for there to be significant grain growth suppression. Pellets infiltrated with SiH_4 or NH_3 alone show no evidence of grain growth suppression while the pellets infiltrated with both SiH_4 and NH_3 exhibit a graded microstructure. SEM images of these samples indicate that the thickness of each region of microstructure is dependent on the amount of SiH_4 used during infiltration. To theoretically determine the impact of the infiltration process on the microstructure of these pellets, an infiltration model was developed to examine the infiltration of SiH_4 into a porous alumina perform.[22]

One of the most interesting findings of this research is our ability to correlate the observed microstructure

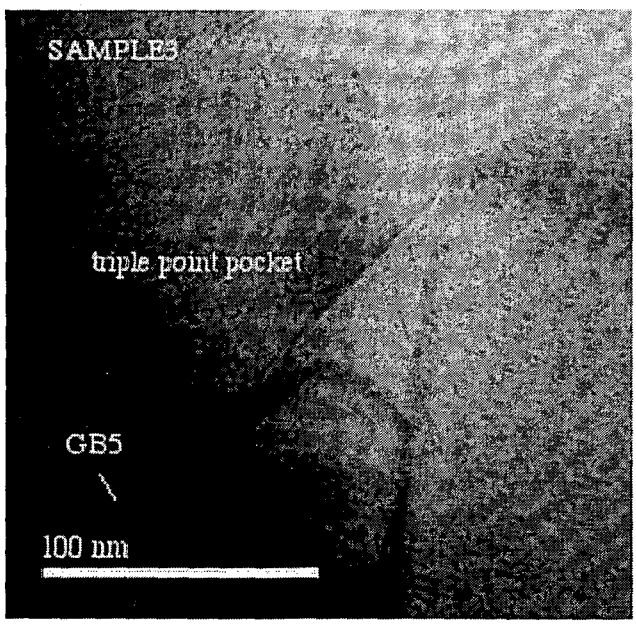

Figure 9. A TEM image taken at the Max Planck Institute shows the presence of a glassy phase at a grain boundary junction.

present in various regions of the pellet with silicon content throughout the pellet. In this study we hypothesized that abnormal grain growth occurred in regions of the sample where the solubility limit of the silicon in alumina had been exceeded. Unfortunately, there is a lack of published solubility data for glass-forming elements in alumina. Two recent reports by Baik suggest that the solubility limit for silica in alumina (in cationic ppm) is 200 ppm at 1700 °C.[24] Researchers at the Max Planck Institute have determined that a concentration greater than 60 ppm of silicon along alumina grain boundaries results in glass formation.[25] By using our infiltration model in conjunction with the microstructural profile obtained form SEM results, the solubility limit for Si at the alumina grain boundaries in this study can be determined as well a information about the quantity of Si_3N_{4y} needed to suppress grain growth in the infiltrated alumina. During Si_3N_{4y} infiltration, the pellets are exposed to a controlled NH_3 and SiH_4 atmosphere. The gases quickly penetrate the porous alumina pellet and react to form a solid product along the pore walls. The formation of solid product diminishes the concentration of reactive gases, and thus depletes the supply of gaseous infiltrant available to diffuse into the remainder of the pellet. Experimental data show that the reaction rate for the deposition of Si_3N_{4y} in our system is first order with respect to the SiH-gas concentration.[26,27,28] Therefore, the SiH concentration is the rate limiting critical

variable to monitor. Using the result of the infiltration model developed in our previous work, the gaseous silicon concentration as a function of depth into the pellet can be determined. From other deposition and compositional parameters associated with the pellet, the Si content in the pellet as a function of depth can be determined. By correlating the Si content with microstructural observations of abnormal, suppressed and normal growth regions, we can obtain numerical limits on the critical value of the concentration of Si necessary to produce abnormal grain growth. We obtain a value of ~70 ppm for the critical concentration (above which abnormal grain growth results). This value is consistent with the values reported by Baik and Rüehle (200 and 60 ppm, respectively).[24, 25] This value was confirmed for many samples, and for a variety of deposition conditions.

It is important to consider the role of nitrogen as well as silicon: suppressed grain growth cannot be attributed to merely the presence of Si below its solubility limit. Our research has provided us which significant insight into the location and role of N in grain growth suppression. As previously mentioned, experimental data suggest that N is necessary for grain growth suppression, and previously published XPS data indicate that the material deposited in our CVD/CVI reactor is sub-stoichiometric silicon nitride. We suggest that some of the nitrogen that is introduced into the sample during deposition is released during the final sinter, while the remaining nitrogen in these infiltrated pellets diffuses a short distance into the alumina grains and associates with the alumina grain boundaries. We estimate that typical diffusion distances are on the order of 1 to 100 nm into the alumina grain. These assumptions imply that extremely small concentrations of Si and N atoms within the alumina grain boundaries are responsible for the suppression of grain growth observed. We have developed and applied theoretical models of both oxidation of the Si_3N_4 and diffusion of nitrogen in oxides to validate our assumptions that a very small amount of Si and N along the grain boundaries could be responsible for the reduction in grain growth.

Silicon nitride oxidation rates can be estimated from available data.[29] This information was used to predict the time required to oxidize a 4 nm thick layer of Si_3N_4 as a function of temperature.[23] These results are shown in Fig. 10. It should be noted that Si_3N_4 oxidizes very rapidly at the elevated temperature used for the final sinter in these studies. It therefore appears likely that some quantity of the nitrogen within the infiltrated specimens is released during thermal processing. However, as previously mentioned, microstructural results suggest that N plays a role in the development of grain boundary morphology (i.e. acting in consort with Si to suppress grain growth.) so not all of the nitrogen can leave areas on or near alumina grain boundaries. This requires that nitrogen atoms diffuse slowly enough to travel only a short distance into the alumina grains but fast enough to move a significant amount of

nitrogen away from the grain boundaries (which is presumably where the oxidation of the N would occur). For this study, the acceptable range for the nitrogen diffusion was found to be from $1(10^{-15}) < D_N < 1(10^{-13})$ cm^2/s. Based on our experiments and published data a description of microstructural evolution and grain growth in the CVI Si_3N4_y/Al_2O_3 system is given below:

1. A silicon-rich silicon nitride is deposited on the particle surfaces (i.e., on future grain boundaries and junctions).
2. As firing begins some N and Si diffuse short distances into adjacent Al_2O_3 grains. Some nitrogen gas evolves and leaves behind SiO_2, a known contributor to abnormal grain growth.
3. Abnormal grain growth occurs only in the areas where the concentration of silica has exceeded the critical value for the formation of a glassy-phase along the grain boundaries.
4. Suppressed grain growth occurs only in the region where silicon nitride is able to influence grain boundary mobility and the concentration of silica has not exceeded the critical value for the formation of a glassy-phase along the grain boundaries.
5. Normal grain growth occurs in regions where the concentration of the infiltrant is essentially non-existent.

In summary, suppressed grain growth only occurs in samples which have been infiltrated with both Si and N precursors, and regions of abnormal grain growth were only observed in samples in which the infiltrant contained some amount of Si and which were sintered in air above 1600 °C. Our observations indicate that deposited Si_3N_{4y} significantly reduces grain growth in Al_2O_3 and that the concentrations of Si and N which are necessary for this suppression to occur are well below the respective solubility limits in Al_2O_3. We therefore conclude that solute drag of both N and Si are responsible for grain growth suppression.

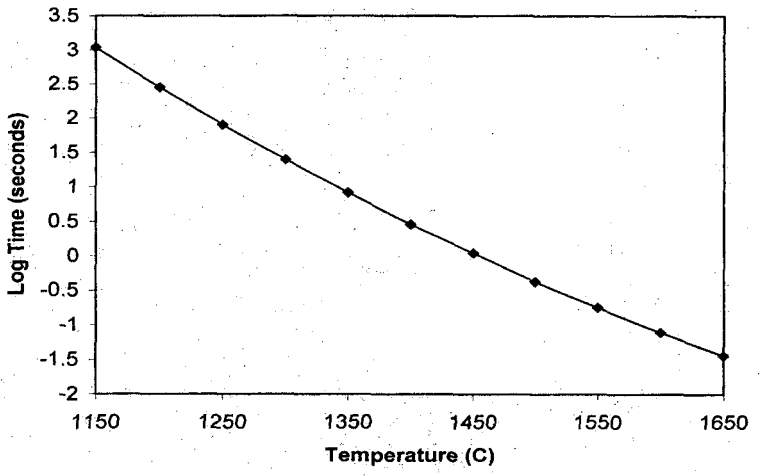

Figure 10. The time required to oxidize a 4 nm thick layer of Si_3N_4 as a function of temperature.

B.2 Work in the Nanoscale System

We have continued our study of grain growth suppression in nano-size alumina powders. Here, silicon nitride infiltration also shows evidence of reduced grain growth, with a 50% reduction in grain size (0.98 compared with Si_3N_{4y}, compared with 1.9 μm for the control). Preliminary microhardness measurements indicate a significant increase in hardness: from 5.77 GPa$\sqrt{m}$, to ~17.6 GPa$\sqrt{m}$ for the control and an "average" infiltrated sample, respectively.

SEM images for this infiltrated nanophase pellets differ significantly from those of the sub-micron pellets. Instead of observing a microstructure with 3 distinct regions, SEM images of nanophase pellets show a microstructure of uniform grain size throughout the pellet; no abnormal grain growth is observed in either the control or sample pellets. We believe that differences in starting material phase and chemical composition, along with differences in processing can explain the observed differences in microstructure. Table I summarizes the salient differences between the nano and submicron starting powders, and their subsequent processing routes.

As found in this study, and by other researchers[24,25] the critical concentration of Si to initiate abnormal grain growth is ~70 ppm. Since the starting concentration of Si in the nano-powder is so low (14 ppm), approximately 56 ppm would have to be introduced by the infiltration process to reach this

threshold. Infiltration calculations indicate that this level should only be attained in roughly the first 30 μm of the near surface region, which is consistent with the experimental results. Also note that the final sintering temperatures and processing atmospheres differ significantly for the sub-micron and nano-scale powders. Baik has reported that the formation temperature for aluminosilicate glass in Si doped alumina is 1550 °C.[24] This falls between the temperatures used to process the submicron and nanosized, powders. In addition, the processing environment is likely to contribute to the difference in observed microstructure. Since the nanosize pellets are annealed in vacuum in a high carbon content environment, thermodynamics do not favor nitrogen gas evolution and no silica should be formed. We hope that

Table I. Summary of Powder Characteristics and Sintering Conditions

	Average Particle Diameter (as received)	Si in starting powder (ppm)	Final Sintering Temperature	Final Sintering Atmosphere
Sub-micron	500 nm	35 ppm	1650 °C	Air
Nano-sized	33 nm	14 ppm	1450 °C	Vacuum

additional collaborations with Max Planck Institute will allow us to verify and quantify the presence, quantity and composition of the infiltrated silicon nitride phase in the nanophase pellets.

Preliminary hardness measurements in the nanophase system suggest that only a minimal improvement in hardness and toughness is realized as a result of these infiltrations. Although the infiltrated samples show a 50% reduction in grain size over the control samples (0.98 v. 1.9 mm average grain size), both sets of grain sizes are in the micron-range. We are continuing our work in this area, focussing on the final processing stages (pressing and firing).

B.3 Liquid Phase infiltration into partially sintered Al_2O_3

Our studies on the use of Zr n-propoxide to infiltrate the pore structure of as-pressed submicron grain sized pellets of alumina have been very successful. Grain growth suppression was achieved with zirconia loading down to 1 vol%. During this funding cycle, we have made significant progress in the analysis of our findings in this system, as noted in our previous annual reports. We are in the process of preparing a paper for publication based on this analysis.

During the past funding cycle, we have also initiated work on a new two step reaction and sintering process to form SiC within Al_2O_3. In these experiments, pellets with a starting density of ~55% are formed by pressing and firing submicron powder Al_2O_3at 1350 °C. Pellets are then infiltrated with TEOS (tetraethyloxysilane) (liquid) and fired at approximately 950 °C in propene gas. Effective pyrolysis of the propene, and subsequent reaction with the Si in the TEOS produces the desired SiC within the pellet. The pellet is then fired in an inert (oxygen-free) environment to produce a fully dense material.

X-ray diffraction has established the existence of SiC within the sample. SEM studies have determined that the SiC forms either, at grain junctions or along,grain boundaries, depending on the exact processing route. SiC along the grain boundaries was found to be less effective than SiC at grain junctions in suppressing Al_2O_3 grain growth. Figure 11 (a) and (b) show SEM images of an Al_2O_3 sample with SiC along the grain boundaries.

It is clear from the initial results that the combination of liquid and vapor infiltration suppresses grain growth. This procedure must be adjusted further to minimize grain growth. In ongoing work on this project, the SiC infiltration process is also being expanded to nanometer pellets.

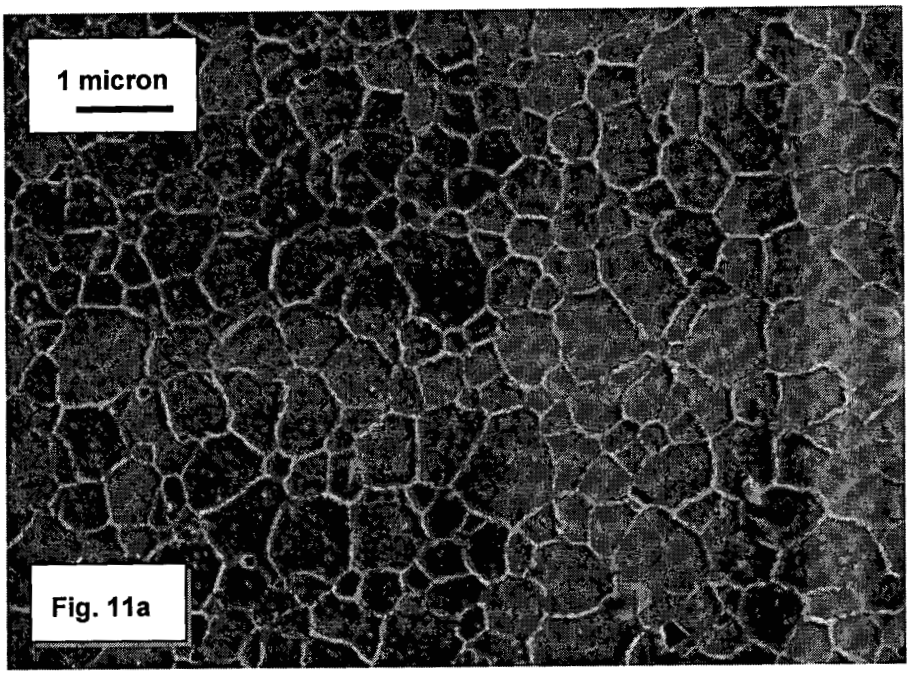

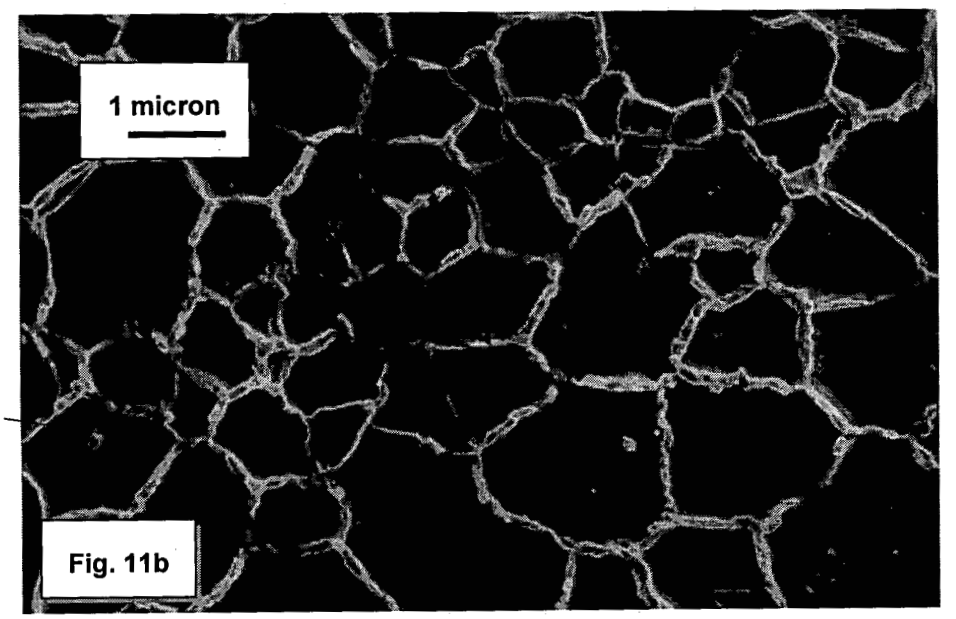

SiC at Boundaries

Figure 11 a) and b) SEM images of an Al_2O_3 sample with SiC along the grain boundaries

C. Conclusions

The work summarized here represents significant and exciting advances in the area of particle coalescence and microstructure evolution in nanosized ceramics. I am grateful to the U.S. Department of Energy for funding of this work.

D. Personnel

- Graduate Student: Deborah M. Vernon - Graduated w/ Ph.D. January 2001. Thesis Title: "Infiltration Techniques for Suppressing Grain Growth During the Densification of Submicron and Nanophase Alumina Composites".

- Undergraduate Student: Elizabeth K. Reilly '01 - Senior Thesis Title: " Combined Liquid and Vapor Infiltration Techniques for Grain Growth Suppression in Nanophase Alumina Compacts

- Undergraduate Student: Alexandra Sullivan '02 – Studied a variety of liquid and gas phase infiltration routes.

References

[1] **J. Rankin,** "*In Situ* TEM Heating of Nanosized ZrO_2", *J. Am. Ceram. Soc.,* **82,** 1560-64 (1999).

[2] **J. Rankin** and B.W. Sheldon, "Surface Roughening and Unstable Neck Formation in Faceted Particles, I: Experimental Results and Mechanisms", *J. Am. Ceram. Soc.,* **82,** 1868-72 (1999).

[3] B.W. Sheldon and **J. Rankin,** "Surface Roughening and Unstable Neck Formation in Faceted Particles, II: Mathematical Modelling", *J. Am. Ceram. Soc.,* **82,** 1873-81 (1999).

[4] S. Iijima, "Electron Microscopy of Small Particles", *J. Electron Microsc.*, **34,** 249 (1985).

[5] J. Rankin, "*In Situ* TEM Sintering of Nanoscale Ceramic Oxide Particles", *Mater. Sci. Eng.,* **A204,** 48 (1995).

[6] W.K. Burton, N. Cabrera, and F.C. Frank, "The growth of crystals and the equilibrium structure of their surfaces", *Phil. Trans. R. Soc.*, **243A,** 299-358 (1951).

[7] W.W. Mullins and G.S. Rohrer, "Nucleation Barrier for Volume-Conserving Shape Changes of Faceted Crystals", *J. Am. Ceram. Soc.,* **83,** 214-16 (2000).

[8] P. Wynblatt and N.A. Gjostein, "Particle Growth in Model Supported Metal Catalysts – I. Theory", *Acta. Metall.*, **24,** 1165-74 (1976).

[9] I.M. Lifshitz and V.V. Slyozov, "The Kinetics of Precipitation from Supersaturated Solid Solutions", *J. Phys. Chem. Solids*, **19,** 35-50 (1961).

[10] C. Wagner, "Theorie der Alterung von Niederschlagen durch Uml sen", *Z. Electrochem.*, 65, 581-91 (1961).

[11] P.W. Voorhees, "Ostwald Ripening of Two-Phase Mixtures", *Annu. Rev. Mater.* Sci., **22,** 197-215 (1992).

[12] L.-Q. Chen and D. Fan, "Computer Simulation Model for Coupled Grain Growth and Ostwald Ripening - Application to Al2O3 - ZrO2 Two Phase Systems", *J. Am. Ceram. Soc.,* **79,** 1163-68 (1996).

[13] B.W. Sheldon and **J. Rankin,** "Step Energy Barriers and Particle Shape Changes during the Coarsening of Faceted Particles", J. Am. Ceram. Soc. **85** 683-90 (2002).

[14] H.C Choi, A.F. Schwartzman, and K.S Kim, "Experimental deformaiton mechanics of materials from their near-atomic-resolution defect images". Mat. Res. Symp. Proc. Vol. 239, pp. 419-424 (1992).

[15] R.C. Picu, K.S. Kim and R. J. Clifton, "Lomer dislocation core structure in silicon-germanium", in preparation.

[16] R.C. Picu and K.S. Kim, "Dilatation of a Lomer dislocation core in silicon", in preparation.

[17] M.J. Kelley, "Two Models for Edge-Energy and Their Effects on Edge and Surface Minimizing Shapes", *Scripta Met.* **33** (9), 1493 (1995).

[18] C-Z. Dong, et al, "Microscopic Aspects of Faceting Induced by Ultrathin Metal Films: A Comparison of Pd/W(111) and Pd/Mo(111)", in Xie et. al. editors, The Structure of Surfaces IV, 1984..

[19] S. Ijima, "Fine Particles of Silicon. I. Crystal Growth of Spherical Particles of Si", **26**(3) 357 (1987).

[20] R. Uyeda, "Studies of Ultrafine Particles in Japan: Crystallography. Methods of Preparation and Technological Applications", in: *Progress in Materials Science*, **35,** 1 (1991).

[21] R. Miller and R. Phillips, "Critical analysis of local constitutive models for slip and decohesion", *Phil. Mag. A* **73,** 803-826 (1996).

[22] Deborah M. Vernon, **Janet Rankin,** Christine Caragianis-Broadbridge, and Bruce Laube, "A Processing Route to Control Grain Growth in Submicron Alumina Compacts", *J. Am. Ceram. Soc.* **82** , 2969 (1999).

[23] Deborah M. Vernon, "Infiltration Techniques for Suppressing Grain Growth During the Densification of

Submicron and Nanophase Alumina Composites", PhD Thesis, Brown University (2001).

[24] a) S.I Bae and S. Baik, "Determination of Critical Concentrations of Silica and/or Calcia for Abnormal Grain Growth in Alumina", *J. Am. Ceram. Soc.* **76**, 1065 (1993).

b) J.H. Yoo, J.C. Nam, and S. Baik, Quantitative Evaluation of Glass Forming Impurities in Alumina", *J. Am. Ceram. Soc.* **2**, 2233 (1999).

[25] Manfred Ruehle, private communication (2000).

[26] C. E. Morosanu, "The Preparation, Characterization and Application of Silicon Nitride Thin-films", *Thin Solid Films*, **65**, 171 (1980).

[27] F.S. Lauten, "Chemical Vapor Deposition of Polycrystalline Si_3N_4 Films at Low Temperatures", Ph.D. Thesis (1996) Brown University, Providence, RI

[28] F.S. Lauten, J. Rankin, and B.W. Sheldon, "Nucleation and Growth of Polycrystalline Si_3N_4 During Chemical Vapor Deposition", in Silicon Nitride Ceramics - MRS Proceedings, Vol. 287, ed. by I.-W. Chen et. al., (Materials Research Society, Pittsburgh, PA., 1993), p. 315.

[29] N.S. Jacobson, "Corrosion of Si-Based Ceramics in Combustion Environments", *J Am Ceram Soc.* **76,** 3 (1993).